Impaired gp100-Specific CD8+ T-Cell Responses in the Presence of Myeloid-Derived Suppressor Cells in a Spontaneous Mouse Melanoma Model

David G. Mairhofer[1], Daniela Ortner[1], Christoph H. Tripp[1,2], Sandra Schaffenrath[1,2], Viktor Fleming[1,3], Lukas Heger[1,3], Kerstin Komenda[1], Daniela Reider[1,2], Diana Dudziak[3], Suzie Chen[4], Jürgen C. Becker[5], Vincent Flacher[1,6] and Patrizia Stoitzner[1]

Murine tumor models that closely reflect human diseases are important tools to investigate carcinogenesis and tumor immunity. The transgenic (tg) mouse strain tg(Grm1)EPv develops spontaneous melanoma due to ectopic overexpression of the metabotropic glutamate receptor 1 (Grm1) in melanocytes. In the present study, we characterized the immune status and functional properties of immune cells in tumor-bearing mice. Melanoma development was accompanied by a reduction in the percentages of CD4+ T cells including regulatory T cells (Tregs) in CD45+ leukocytes present in tumor tissue and draining lymph nodes (LNs). In contrast, the percentages of CD8+ T cells were unchanged, and these cells showed an activated phenotype in tumor mice. Endogenous melanoma-associated antigen glycoprotein 100 (gp100)-specific CD8+ T cells were not deleted during tumor development, as revealed by pentamer staining in the skin and draining LNs. They, however, were unresponsive to *ex vivo* gp100-peptide stimulation in late-stage tumor mice. Interestingly, immunosuppressive myeloid-derived suppressor cells (MDSCs) were recruited to tumor tissue with a preferential accumulation of granulocytic MDSC (grMDSCs) over monocytic MDSC (moMDSCs). Both subsets produced Arginase-1, inducible nitric oxide synthase (iNOS), and transforming growth factor-β and suppressed T-cell proliferation *in vitro*. In this work, we describe the immune status of a spontaneous melanoma mouse model that provides an interesting tool to develop future immunotherapeutical strategies.

INTRODUCTION

Clinically relevant animal models of melanoma that mimic the human situation are crucial for investigations of tumor etiology and immunology. Chen *et al.* (1996) came across a spontaneous melanoma model when they tried to generate a

[1]Department of Dermatology and Venereology, Medical University of Innsbruck, Innsbruck, Austria; [2]Oncotyrol, Center for Personalized Cancer Medicine, Innsbruck, Austria; [3]Department of Dermatology, Laboratory of DC-Biology, Friedrich-Alexander University of Erlangen-Nürnberg, University Hospital of Erlangen, Erlangen, Germany; [4]Department of Chemical Biology, Lab for Cancer Research, Rutgers University, Piscataway, New Jersey, USA and [5]Department for Translational Dermato-Oncology, Center for Medical Biotechnology, University Hospital Essen, Essen, Germany

Correspondence: Patrizia Stoitzner, Department of Dermatology and Venereology, Medical University of Innsbruck, Anichstrasse 35, Innsbruck A-6020, Austria. E-mail: patrizia.stoitzner@i-med.ac.at

[6]Current address: CNRS UPR 3572, Laboratory of Immunopathology and Therapeutic Chemistry/Laboratory of Excellence MEDALIS, Institut de Biologie Moléculaire et Cellulaire, Strasbourg, France.

Abbreviations: BMDCs, bone marrow-derived dendritic cells; gp, glycoprotein; grMDSCs, granulocytic myeloid–derived suppressor cells; Grm1, metabotropic glutamate receptor1; iNOS, inducible nitric oxide synthase; LN, lymph node; MDSC, myeloid-derived suppressor cell; moMDSCs, monocytic myeloid–derived suppressor cells; qPCR, quantitative PCR; tg, transgenic; TGF-β, transforming growth factor-β; Tregs, regulatory T cells

Received 18 December 2014; revised 1 June 2015; accepted 11 June 2015; accepted article preview online 29 June 2015; published online 30 July 2015

mouse with adipocyte dysfunction. This strain, named LLA-TG3, possessed multiple tandem insertions of a transgene in the gene *Grm1* encoding the metabotropic glutamate receptor 1 (Grm1), resulting in systemic overexpression. This led to the persistence of melanocytes in skin areas without fur, e.g. ear and tail skin, followed by hyperproliferation and subsequent melanoma development (Chen *et al.*, 1996; Cohen-Solal *et al.*, 2001). The significance of Grm1 in tumorigenesis was confirmed by the generation of the tg(Grm1)EPv mouse model, in which overexpression of Grm1 is driven by the melanocyte-specific dopachrome tautomerase promoter (Pollock *et al.*, 2003). These mice spontaneously develop melanoma with a 100% penetrance at the age of 4–6 months in skin regions such as ear and tail skin. Tumors in tg(Grm1) EPv mice do metastasize, as the presence of melanoma cells in lymph nodes (LNs) has already been reported (Pollock *et al.*, 2003). Grm1-positive cells could also be detected in lymphatic organs and in lung as well as liver; however, most of these cells were non-pigmented (Schiffner *et al.*, 2012). The relevance of this pathway for human tumorigenesis was substantiated by the fact that >60% of human melanoma samples overexpress Grm1 (Namkoong *et al.*, 2007).

Cancer immunosurveillance as proposed in 1957 by Burnet controls both initial steps of carcinogenesis and cancer
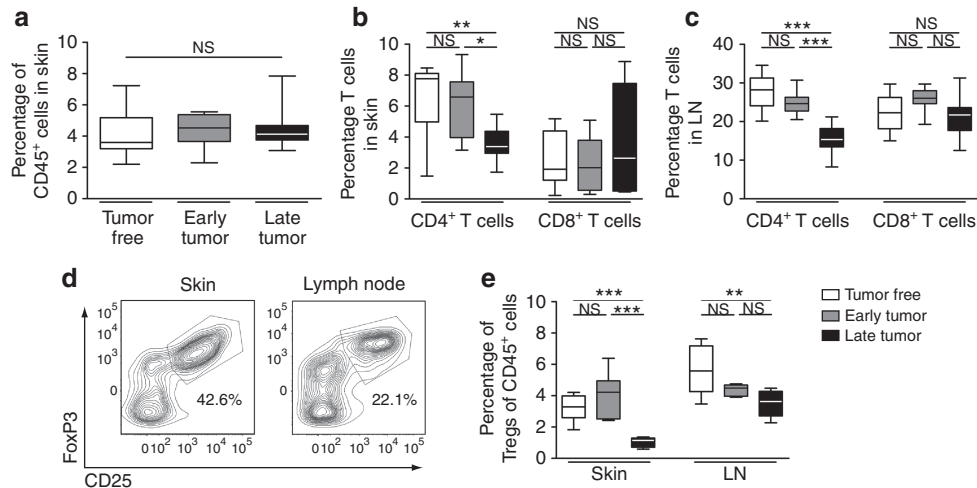
Figure 1. The percentages of CD4+ T cells and Tregs are reduced in late-stage tumors of tg(Grm1)EPv mice. Cell suspensions from the skin and draining lymph nodes (LNs) of tumor-free, early-stage, and late-stage tumor tg(Grm1)EPv mice were analyzed by flow cytometry. (**a**) Percentages of CD45+ leukocytes are shown after pregating on viable cells ($n = 14$ mice). For all further analyses, the percentages of cells were calculated based on CD45+ viable cells. (**b** and **c**) CD4+ and CD8+ T cells were analyzed in (**b**) the skin ($n = 8$ mice) and (**c**) the draining LNs ($n = 15$ mice). (**d**) Representative FACS plots for FoxP3+ CD25+ Tregs in the skin and draining LNs of tumor-free mice. (**e**) Summary graph for the percentages of FoxP3+ CD25+ Tregs in the skin and draining LNs ($n \geqslant 8$ mice).

progression (Burnet, 1957). The immune system is able to recognize and eliminate transformed cells, as demonstrated by enhanced susceptibility to cancer when the immune system is impaired (Dunn et al., 2002). The balance between effective tumor immunity and tumor escape mechanisms decides on the elimination or progression of cancer (Schreiber et al., 2011). Cytotoxic effector cells such as T and natural killer cells infiltrate tumor tissue to fight tumor cells (Vesely et al., 2011; Gajewski et al., 2013). One prerequisite for effective anti-tumor immunity is the presentation of antigens by tumor cells and their recognition by infiltrating cytotoxic CD8+ T cells. A problem encountered with many tumor-associated antigens is that they are poorly immunogenic non-mutated self-antigens. A reason for their poor immunogenicity is tolerance induction associated with the deletion or anergy of self-reactive CD8+ T cells during tumorigenesis (Willimsky and Blankenstein, 2007). In addition, tumors employ a complex immunosuppressive network to escape immune recognition. Suppressive cells, such as regulatory T cells (Tregs) and myeloid-derived suppressor cells (MDSCs), infiltrate tumors and prevent anti-tumor immune responses (Nishikawa and Sakaguchi, 2010; Gabrilovich et al., 2012). These various immune evasion mechanisms eventually result in an impaired function of cytotoxic CD8+ T cells and natural killer cells translating in a poor prognosis for the patients (Schreiber et al., 2011; Motz and Coukos, 2013). Despite this, CD8+ T cells specific for tumor-associated self-antigens, such as glycoprotein 100 (gp100), tyrosinase, and MART, do exist in patients with malignant melanoma (Bakker et al., 1994; Kawakami et al., 2000; Boon et al., 2006). For this reason, clinical studies are using melanosomal antigens for vaccination approaches (Rosenberg et al., 2004).

In the present study, we characterized the immunological features of a spontaneous mouse melanoma model based on Grm1 overexpression that can also be observed in about 60%

of human melanoma samples. Our results suggest that tumors grow progressively despite the presence of activated T cells. We found possible explanations for impaired tumor immunity, including gp100-specific CD8+ T-cell anergy and the infiltration of immunosuppressive MDSCs into the tumor microenvironment.

RESULTS

The percentages of CD4+ T cells and Tregs are reduced in late-stage tumors of tg(Grm1)EPv mice

The immunological status of the tg(Grm1)EPv mouse was hitherto unknown; hence, we characterized the immune cells present in tumor tissue and draining LNs. For this purpose, we compared tumor-free mice (2–3 months of age) with mice bearing early-stage (5–6 months) and late-stage tumors (8–9 months; Supplementary Figure S1 online). Immunofluorescence stainings of late-stage tumor sections revealed that CD4+ and CD8+ T cells were present in the tumor and that a proportion of CD4+ T cells co-expressed FoxP3-a marker for Tregs (Supplementary Figure S2 online).

For quantification of immune cells present in tumor-free and tumor-bearing mice, ear skin and draining LNs were enzymatically digested, and CD45+ cells were analyzed by flow cytometry. Because tumor growth in tg(Grm1)EPv mice occurs progressively over several months, we also monitored young (2–3 months) and old (8–9 months) C57BL/6 mice in order to rule out that these observed changes were not solely caused by aging (Supplementary Figure S3 online).

There was no change in the overall percentages of CD45+ cells in the skin of tumor-free, early-stage, and late-stage tumor mice (Figure 1a), similar to what we observed in C57BL/6 mice (Supplementary Figure S3a online). Less CD4+ T cells were present in late-stage tumors (Figure 1b), a feature that was clearly absent from old C57BL/6 mice (Supplementary Figure

S3b online). Cutaneous CD8$^+$ T cells were unaltered by tumor development (Figure 1b), despite showing a slight increase over aging in C57BL/6 mice (Supplementary Figure S3b online). However, in LN draining either late-stage tumor of tg(Grm1)EPv mice (Figure 1c) or the skin of aged C57BL/6 mice (Supplementary Figure S3c online), we observed a comparable reduction in CD4$^+$ T cells, suggesting that this change might be age related. In addition, we were able to detect CD4$^+$ T cells expressing the Treg marker FoxP3 in the skin and lymphoid tissue of tg(Grm1)EPv mice (Figure 1d). The percentages of Tregs in the total CD45$^+$ cell pool were reduced in late-stage tumor tissue and the draining LNs (Figure 1e), whereas these proportions remained the same in young and old C57BL/6 mice (Supplementary Figure S3d online). Altogether, our data suggest tumor-related reduction of CD4$^+$ T cells including Tregs in tumor tissue.

Activated T cells are present in late-stage tumor mice and can produce IFN-γ

Because of the fact that percentages of T cells differed between tumor-free and late-stage tumor tg(Grm1)EPv mice, we assessed the phenotype and functional properties of T cells in draining LNs of these mice. Tumor development was accompanied by a significant upregulation of the activation marker CD44 and a reduction in the homing receptor L-selectin (CD62L) on CD4$^+$ and CD8$^+$ T cells, reflecting enhanced differentiation into CD44^{hi} CD62L^{low} effector memory T cells (Figure 2a). In addition, more T cells upregulated the activation marker CD69 in draining LNs when compared with tumor-free mice (Figure 2b). Next, we determined whether tumor formation would alter the ability of T cells to produce the cytokine IFN-γ. For this purpose, LN cell suspensions were restimulated *in vitro* with antibodies against CD3 and CD28. CD4$^+$ T cells showed little IFN-γ, and production was unchanged upon tumor development. In contrast, more CD8$^+$ T cells produced IFN-γ in draining LNs of late-stage tumor mice (Figure 2c). Although similiar activation patterns were detected in LNs of aged C57BL/6 mice indicating possible age-related effects (Supplementary Figure S4 online), it is still interesting to note that activated and functional T cells are present in the draining LNs of tumor-bearing tg(Grm1)EPv mice.

Endogenous gp100-specific CD8$^+$ T cells are present in tumor mice but are functionally impaired upon antigen-specific restimulation

Despite the presence of activated T cells in tumor-bearing tg(Grm1)EPv mice, tumor growth cannot be controlled. To better understand the mechanisms behind impaired tumor immunity, we investigated T cells by pentamer staining with a focus on the presence and functional properties of gp100-specific CD8$^+$ T cells (Figure 3a). We found that, in the skin and draining LNs of tg(Grm1)EPv mice, the percentages of gp100-specific CD8$^+$ T cells were not affected by tumor development (Figure 3b). In order to test the functional properties of gp100-specific CD8$^+$ T cells, we performed antigen-specific *in vitro* restimulation of total LN cells with a gp100 peptide. The percentages of gp100-responsive CD8$^+$
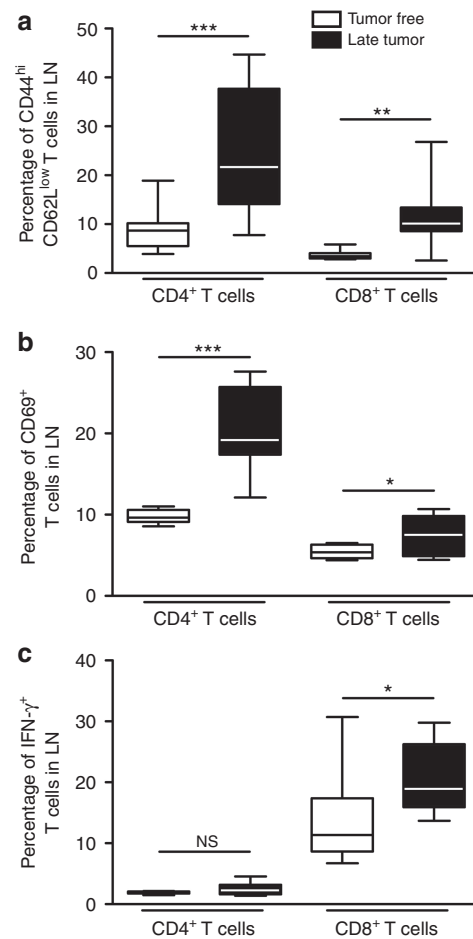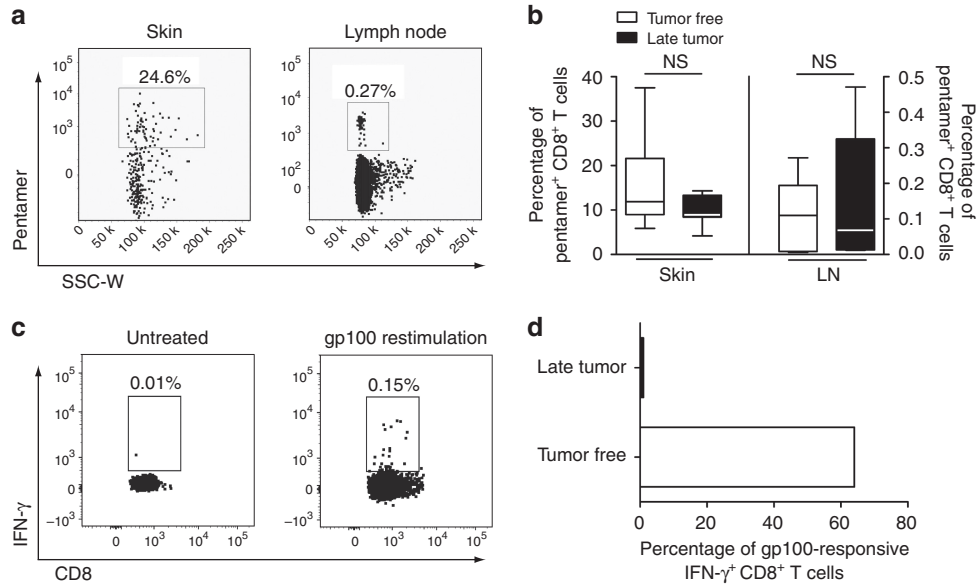
Figure 2. Activated T cells are present in late-stage tumor mice and produce IFN-γ. Cell suspensions from draining lymph nodes (LNs) of tumor-free and late-stage tumor tg(Grm1)EPv mice were analyzed by flow cytometry. All analyses used a pregate on CD45$^+$ viable cells. CD4$^+$ and CD8$^+$ T-cell subsets in draining LNs were analyzed for the following: (**a**) CD44^{hi} CD62L^{low} T cells ($n = 11$ mice) and (**b**) CD69$^+$ activated T cells ($n = 8$ mice). (**c**) IFN-γ-producing T cells were analyzed after restimulation of LN cells with antibodies against CD3 and CD28 for 48 h ($n \geqslant 6$ mice).

T cells were determined by comparing the proportion of CD8$^+$ T cells producing IFN-γ upon gp100-peptide restimulation related to the proportion of CD8$^+$ T cells labeled by major histocompatibility complex I/gp100 pentamer. This calculation was necessary because IFN-γ–producing CD8$^+$ T cells downregulate their TCR, which can therefore no longer be detected in a reliable way by pentamer staining. In tumor-free tg(Grm1)EPv mice, 60% of pentamer$^+$ CD8$^+$ T cells produced IFN-γ, whereas T cells in late-stage tumor mice were incapable of producing IFN-γ (Figure 3c and d). These data suggest that, in late-stage tumor tg(Grm1)EPv mice, gp100-specific CD8$^+$ T cells are anergic to the melanocyte-derived antigen gp100.

MDSCs accumulate in the skin and draining lymph nodes of late-stage tumor mice

The reduction of Tregs in late-stage tumors of tg(Grm1)EPv mice suggested a negligible role for inhibition of anti-tumor

Figure 3. Endogenous glycoprotein 100 (gp100)-specific CD8+ T cells are present in late-stage tumors but are functionally impaired upon antigen-specific restimulation. Cell suspensions from the skin and draining lymph nodes (LNs) of tumor-free and late-stage tumor tg(Grm1)EPv mice were analyzed by flow cytometry for gp100-specific CD8+ T cells. All analyses used a pregate on CD45+ viable cells. (**a**) Representative FACS plots from a tumor-free tg(Grm1)EPv mouse for pentamer+ CD8+ T cells in the skin and draining LNs, pregate on viable CD8+ T cells. (**b**) Summary graph for pentamer+ CD8+ T cells in the skin and draining LNs ($n \geqslant 9$ mice). (**c**) Representative FACS plots from a tumor-free tg(Grm1)EPv mouse for IFN-γ production of CD8+ LN cells cultured without (untreated) or with gp100 peptide for 48 h. (**d**) Summary graph for gp100-responsive IFN-γ+ CD8+ cells calculated as following: ((mean of IFN-γ+ CD8+ cells restimulated with gp100 peptide) − (mean of IFN-γ+ CD8+ cells cultured without gp100 peptide))/(mean of unstimulated pentamer+ CD8+ cells), $n \geqslant 4$ mice.

immune responses by this cell type. Another population of immunosuppressive cells, namely MDSCs, are capable of suppressing immune responses against tumors, thereby allowing tumor escape (Gabrilovich *et al.*, 2012). We investigated CD11b+ Gr-1+ MDSCs in the skin and draining LNs of tumor-free, early-stage, and late-stage tumor mice. In the skin, MDSCs accumulated in late-stage tumors, and, a similar trend was observed in the tumor-draining LNs, albeit not as pronounced as in the skin (Figure 4a and b). In an effort to characterize CD11b+ Gr-1+ MDSC subsets, we analyzed the percentages of CD11b+ Gr-1inter Ly-6Chigh monocytic MDSCs (moMDSCs) and CD11b+ Gr-1high Ly-6Clow granulocytic MDSCs (grMDSCs) in the skin and draining LNs of tumor-free and late-stage tumor mice. Tumor development led to an accumulation of both MDSC subsets in the skin and draining LNs of tg(Grm1)EPv mice (Figure 4c and d). We examined additional markers on MDSCs and detected higher levels of M-CSF receptor (CD115) and major histocompatibility complex class II on moMDSCs than on grMDSCs (Supplementary Figure S5 online). In order to rule out that MDSC infiltration was age related, we analyzed both MDSC subsets in young and old C57BL/6 mice. No MDSC accumulation was detected in both the skin and draining LNs of aged C57BL/6 mice (Supplementary Figure S6 online). Thus, accumulation of CD11b+ Gr-1+ cells in late-stage tumors of tg(Grm1)EPv mice suggested an immunosuppressive tumor microenviroment that favors tumor growth.

MDSCs in the tumor are potent suppressors of T-cell activity
In order to test the capacity of MDSCs to suppress T-cell activity, we flow cytometrically sorted MDSC subsets from the

skin of late-stage tumor tg(Grm1)EPv mice (Supplementary Figure S7a online). We purified gp100-specific CD8+ T cells from pmel-1 mice and cultured them with gp100-peptide–loaded mature bone marrow–derived dendritic cells (BMDCs). The gp100-specific CD8+ T cells proliferated in response to peptide-loaded BMDCs, and the addition of sorted moMDSCs or grMDSCs significantly reduced T-cell proliferation (Figure 5a). The suppression of T-cell function was dependent on the number of MDSCs (Supplementary Figure S7b online).

Next, we attempted to elucidate factors responsible for MDSC-mediated immunosuppression and investigated the expression of Arginase-1 and inducible nitric oxide synthase (iNOS) in moMDSCs and grMDSCs sorted from late-stage tumors. In addition, we examined transforming growth factor-β (TGF-β), a cytokine that is considered to be one of the key immunosuppressive factors released by tumors and MDSCs (Gabrilovich and Nagaraj, 2009). Quantitative PCR (qPCR) analysis of sorted MDSCs from tumors revealed high mRNA levels for all three molecules and low to undetectable levels in tumor cells and non-MDSC immune cells (Figure 5b–d). In addition, we observed different expression patterns in the two MDSC subsets, such that grMDSCs expressed higher mRNA levels of iNOS (Figure 5c) and TGF-β (Figure 5d) but lower levels of Arginase-1 compared with moMDSCs (Figure 5b). This was confirmed by intracellular flow cytometric analysis showing that more grMDSCs were positive for iNOS than for Arginase-1 (Figure 5e–h). From this we conclude that grMDSCs as the predominant immunosupressive population in tumors of tg(Grm1)EPv mice most likely suppress T-cell function by iNOS, TGF-β, and Arginase-1 production.
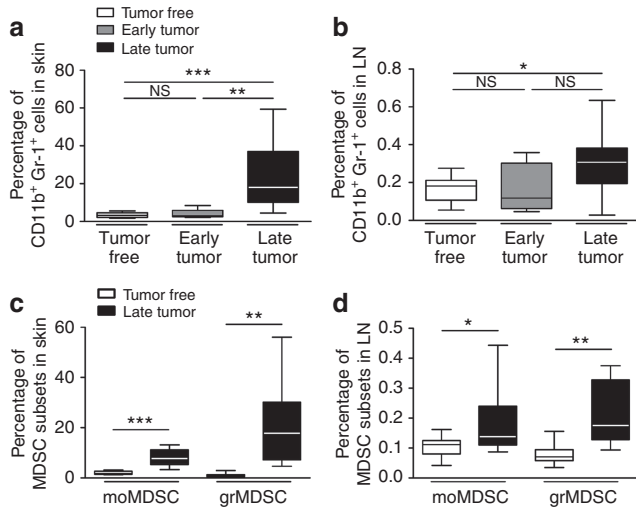
Figure 4. Myeloid-derived suppressor cells (MDSCs) accumulate in the skin and draining lymph nodes (LNs) of late-stage tumor mice. Cell suspensions of tumor-free, early-stage, and late-stage tumor tg(Grm1)EPv mice were analyzed by flow cytometry for the presence of $CD11b^+$ $Gr-1^+$ MDSCs in (**a**) the skin and (**b**) draining LNs ($n = 6$ mice). MDSCs were further subdivided into $CD11b^+$ $Gr-1^{inter}$ $Ly-6C^{high}$ monocytic MDSCs (moMDSCs) and $CD11b^+$ $Gr-1^{high}$ $Ly-6C^{low}$ granulocytic MDSCs (grMDSCs) in tumor-free and late-stage tumor tg(Grm1)EPv mice for (**c**) the skin and (**d**) the draining LNs ($n = 10$ mice). All analyses used a pregate on $CD45^+$ viable cells.

DISCUSSION

Transgenic (tg) mouse models based on genetic aberrations are essential for an improved understanding of melanoma biology and immunology (Becker *et al.*, 2010). Here, we have investigated the immune status of a murine melanoma model based on ectopic overexpression of Grm1 in melanocytes. This overexpression results in spontaneous tumor development and established a link between metabotropic glutamate signaling in melanocytes and melanoma development, reflecting the relevance of this mouse model and the functional importance of the glutamate pathway in cancer (Pollock *et al.*, 2003; Prickett and Samuels, 2012). In line with this, studies on human tumor material revealed that Grm1 is aberrantly expressed in 60% of human melanoma samples (Namkoong *et al.*, 2007). Over the last decade, several studies made use of this murine melanoma model in order to better understand the metastatic behavior of tumors and to test future immunotherapeutical approaches (Marin *et al.*, 2006; Xiao *et al.*, 2011; Schiffner *et al.*, 2012). However, nothing was known about the immune status of these mice. In this work, we describe the composition of immune cells present in the skin and draining LNs of tumor-free and tumor-bearing mice and provide some clues on their functional role in tumor immunity. We observed immunosuppression on two levels: (i) $CD8^+$ T cells seemed to be anergic to the melanoma-associated antigen gp100; (ii) MDSCs with the ability to suppress gp100-specific $CD8^+$ T-cell response represented the dominating immune cell population in late-stage tumor tissue mediating their suppressive effect by iNOS, TGF-β, and Arginase-1 production.

High prevalence of T cells in tumors is an indicator for longer overall survival of advanced-stage melanoma patients (Haanen *et al.*, 2006; van Houdt *et al.*, 2008). Therefore, we characterized the composition of immune cells present in the tumor microenvironment and the draining LNs to which immune cells might relocate. When we investigated the $CD45^+$ cell pool, we observed that the $CD8^+$ T-cell frequencies were not affected by tumor growth, whereas the percentages of $CD4^+$ T cells including Tregs were significantly reduced in late-stage tumor mice. The $CD4^+$ T-cell reduction in the draining LNs was also detectable in aged C57BL/6 mice, indicating an age-related effect on immune cell composition; however, all other alterations in the precentages of immune cells in tg(Grm1)EPv mice were tumor associated. Thus, our findings indicate that early- and late-stage tumors are not infiltrated by T cells correlating with a less immunogenic microenvironment (Gajewski *et al.*, 2013). The observed reduction in Tregs fits to an earlier report on the ret-tg mouse model for melanoma that demonstrated recruitment of Tregs in early-stage tumors followed by a decrease in Tregs in late-stage tumors (Kimpfler *et al.*, 2009). The authors also showed that depletion of Tregs did not delay tumor development, indicating an alternative source of immunosuppression. In contrast, in a transplantable B16 melanoma mouse model, the depletion of Tregs caused a partial regression of established tumors (Klages *et al*, 2010). Hence, the mechanisms of immunosuppression might differ between the various mouse tumor models for melanoma.

The undisturbed tumor growth in the tg(Grm1)EPv mouse model led us to hypothesize that the remaining lymphocytes are compromised in mounting a proper immune response against the tumor. In line with this, studies performed in human melanoma patients and various murine melanoma models suggested that lymphocytes are dysfunctional (Ladanyi *et al.*, 2004; Boon *et al.*, 2006; Ahmadzadeh *et al.*, 2009; Fourcade *et al.*, 2010; Landsberg *et al.*, 2010). Therefore, we characterized the activation status of T cells present in the draining LNs of late-stage tumor mice. These mice showed elevated percentages of $CD44^{hi}$ $CD62L^{low}$ $CD4^+$ and $CD8^+$ T cells. Enhanced activation was further confirmed by higher levels of the early activation marker CD69 on both T-cell subsets. This implied that, similar to the ret-tg melanoma mouse model (Umansky *et al.*, 2008), tumor growth is accompanied by T-cell differentiation into effector memory T cells. In addition, $CD8^+$ T cells from LN draining late-stage tumors were able to produce IFN-γ upon *in vitro* restimulation, indicating that they are not functionally impaired. However, we cannot exclude that aging has some effect due to similar findings in old C57BL/6 mice and reports that showed an activated phenotype in T cells of aged mice (Akbar and Henson, 2011). Nevertheless, the fact that tumor growth cannot be contained by the immune system suggested potent immune escape mechanisms.

Adaptive immunity against the tumor is conducted by antigen-specific T cells. In the case of melanoma, the antigen gp100 is expressed by melanocytes and upregulated during tumor growth. This protein represents a tumor-associated
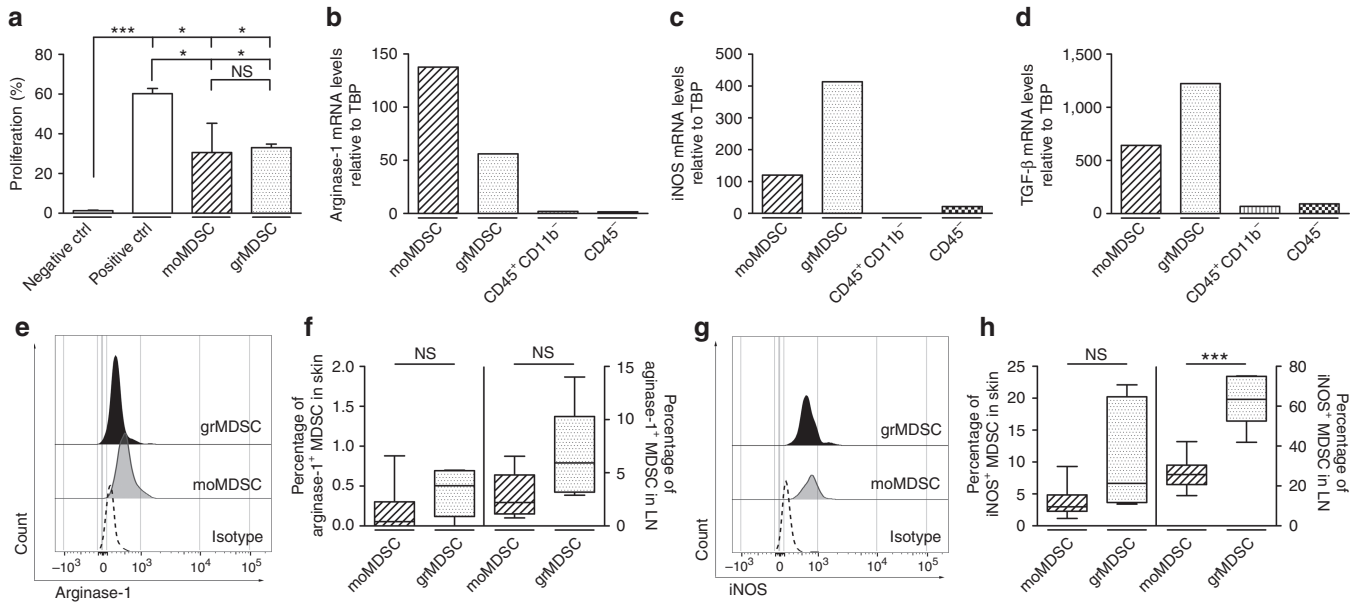
Figure 5. Myeloid-derived suppressor cells (MDSCs) in the tumor are potent suppressors of T-cell activity. Sorted MDSC subsets from ear and tail skin of late-stage tumor tg(Grm1)EPv mice were used to suppress CD8$^+$ T–cell proliferation. (**a**) glycoprotein 100 (gp100)-specific pmel-1 CD8$^+$ T cells (2×10^4) were purified, CFSE-labeled (0.4 μM), and cultured for 3 days together with gp100 peptide–pulsed bone marrow–derived dendritic cells (BMDCs; 1×10^2). Sorted grMDSCs (1×10^4) or moMDSCs (1×10^4) were added to cultures, and proliferation of T cells was measured ($n = 3$ experiments). (**b-d**) Quantitative PCR analysis of sorted granulocytic MDSC (grMDSCs) and monocytic MDSC (moMDSCs) from six late-stage tg(Grm1)EPv mice in comparison with CD45$^-$ tumor cells and CD45$^+$ CD11b$^-$ leukocytes was performed for (**b**) Arginase-1, (**c**) inducible nitric oxide synthase (iNOS), and (**d**) transforming growth factor-β (TGF-β). (**e–h**) Representative histograms from skin MDSCs and summary graphs of the percentages of positive MDSCs in the skin and draining LNs from late-stage tg(Grm1)EPv mice are shown for (**e** and **f**) Arginase-1 and (**g** and **h**) iNOS, ($n = 6$ mice).

antigen that can be recognized by gp100-specific CD8$^+$ T cells (Bakker *et al.*, 1994; Boon *et al.*, 2006; Rizzuto *et al.*, 2009). In tumor-free tg(Grm1)EPv mice, <0.5% of CD8$^+$ T cells were specific for gp100 in the draining LNs as opposed to 10–15% gp100-specific CD8$^+$ T cells in the skin. Tumorigenesis had no effect on the percentages of gp100-specific CD8$^+$ T cells; however, CD8$^+$ T cells from LNs of late-stage tumor mice were unresponsive to restimulation to gp100 peptide *in vitro*. These findings suggest an anergic state due to tolerance induction to the differentiation antigen gp100. Similar to gp100, many tumor-associated antigens are non-mutated self-proteins that represent attractive targets for immunotherapy as they are shared between patients. However, a state of functional tolerance apparently exists (Boon *et al.*, 2006). Nevertheless, it has been reported that immunization with gp100 can induce cytotoxic T-cell responses in murine melanoma models (Overwijk *et al.*, 2003; Xiao *et al.*, 2011) and has been used in clinical trials to treat cancer patients (Rosenberg *et al.*, 2004). In order to generate anti-tumor immune response against gp100, potent immunization approaches need to be employed, such as viral vectors. In the case of the tg(Grm1)EPv mouse model, it has been reported that immunization with viral vectors before tumor onset could fully protect from melanoma development, and a delay in tumor growth could be achieved in tumor-bearing mice (Xiao *et al.*, 2011).

The self-tolerance to gp100 antigen might explain the inability of the immune system to prevent tumor development in the tg(Grm1)EPv mouse; however, in addition, we observed

that the tumor employs another immune escape mechanism to suppress tumor immunity (Gajewski *et al.*, 2013). MDSCs are a heterogeneous population of cells derived from the myeloid lineage endowed with strong immunosuppressive activities. Formation of these cells is triggered under chronic inflammatory conditions or in cancer, where they infiltrate the affected tissue and suppress innate and adaptive immune responses (Gabrilovich and Nagaraj, 2009). In tg(Grm1)EPv mice, few MDSCs were detected in the skin and draining LNs of tumor-free and early-stage tumor mice. However, a strong infiltration of MDSCs could be observed in late-stage tumors. This was not age related as old C57BL/6 mice showed no MDSC accumulation. In addition, a shift toward more grMDSCs as compared with moMDSCs was apparent, mimicking the situation previously described in other murine tumor models and in human cancer patients (Zea *et al.*, 2005; Youn *et al.*, 2008). It has been reported that both subsets efficiently suppress antigen-driven CD8$^+$ T-cell proliferation *in vitro* (Youn *et al.*, 2008). We had similar findings with grMDSCs and moMDSCs sorted from late-stage tumors that proved to be able to suppress gp100-specific CD8$^+$ T-cell proliferation *in vitro*. Arginase-1 and iNOS have been described as key mediators of the suppressive capacity of MDSCs in tumors (Gabrilovich and Nagaraj, 2009). Quantitative PCR analysis of sorted grMDSCs and moMDSCs from tumor tissue of late-stage tg(Grm1)EPv mice revealed high mRNA levels of Arginase-1 and iNOS, and expression was confirmed by flow cytometric analyses. Moreover, TGF-β, a molecule that has been linked to tumor initiation, progression, and metastasis (Gabrilovich and

Nagaraj, 2009), was also elevated at the mRNA level in sorted MDSCs from tumor tissue. Our data suggest that grMDSCs most likely suppress tumor immunity by iNOS, TGF-β, and to a lesser extent with Arginase-1. The high levels of TGF-β produced by grMDSCs but also moMDSCs have an important role in tumor progression as reported earlier (Yang *et al.*, 2010).

Altogether, we describe here the immune status of mice developing melanoma spontaneously due to the ectopic overexpression of Grm1. Despite the presence of activated T cells with memory phenotype, the immune system fails to mount an effective immune response to control melanoma development. The reasons for impaired adaptive immunity are the anergy of melanoma-antigen-associated CD8^{+} T cells and the infiltration of immunosuppressive MDSCs to the tumor microenvironment. This spontaneous mouse melanoma model is highly relevant for research on human melanoma due to the same aberrant overexpression of Grm1, which can be observed in 60% of human melanoma samples (Pollock *et al.*, 2003). The relevance is further substantiated by the fact that the immune composition of tumors is similar to that in humans, reflected by the infiltration of immunosuppressive cells (Senovilla *et al.*, 2012). Taken together, these features make this mouse model an interesting and an important tool to test future immunotherapeutical approaches.

MATERIALS AND METHODS

Mice

Breeding pairs of the tg mouse strain tg(Grm1)EPv (Pollock *et al.*, 2003) were provided by Jürgen C. Becker (Department of Dermatology and Venereology, Medical University Graz, Austria). Tumor-free mice were used before tumor onset (2–3 months) and compared with mice bearing early-stage tumors (5–6 months) and late-stage tumors (8–9 months). C57BL/6 mice were originally derived from Charles River (Sulzfeld, Germany). The T-cell receptor tg pmel-1 mice (Overwijk *et al.*, 2003) were kindly provided by Thomas Tüting (Universitätsklinikum Bonn, Germany). All mouse strains were bred at the animal facility of the Department of Dermatology and Venereology at the Medical University of Innsbruck. All experimental protocols were approved by the Austrian Federal Ministry of Science and Research and performed according to institutional guidelines.

Flow cytometric analyses of the skin and draining LN cell suspensions

Ear skin from tumor-free and tumor-bearing tg(Grm1)EPv mice, as well as C57BL/6 mice, was cut into small pieces and digested with 0.15 mg ml^{-1} Liberase (Roche Diagnostics, Mannheim, Germany) and 0.12 mg ml^{-1} DNAse (Roche) for 45 min at 37 °C and pressed through 100-μm cell strainers (BD Biosciences, Franklin Lakes, NJ). Auricular LNs from tumor-free and tumor-bearing tg(Grm1)EPv mice, as well as C57BL/6 mice were digested with 0.125 mg ml^{-1} collagenase D (Roche) and 0.12 mg ml^{-1} DNAse (Roche) for 25 min at 37 °C and pressed through 100-μm cell strainers (BD Biosciences). All antibody staining steps were performed for 15 min at 4 °C. Nonspecific FcR-mediated antibody staining was blocked by incubation for 15 min with anti-CD16/32 Ab (2.4G2, in-house from hybridoma supernatant and BD Biosciences). For intracellular IFN-γ production, LN cells were restimulated with 3 μg ml^{-1} anti-CD3

(clone 17A2, BD Biosciences) plus 3 μg ml^{-1} anti-CD28 (clone 37.51, BD Biosciences) for 48 h at 37 °C. Cytokine release was blocked with 1 μg ml^{-1} Brefeldin A (BD Biosciences) during the last 4 h of restimulation. The cells were fixed using the BD Biosciences Cytofix/Cytoperm Kit (BD Biosciences) according to the manufacturer's protocol. FoxP3 staining was performed with the FoxP3/ transcription factor staining buffer set from eBioscience (San Diego, CA). The following antibodies were used: anti-Ly-6C-FITC (clone AL-21), anti-IFN-γ-APC (clone XMG1.2), and anti-CD3-FITC (clone 17A2) all from BD Biosciences; anti-CD45-FITC (clone 30.F11), anti-FoxP3-PE (clone FJK-16s), and anti-iNOS-PE (clone CXNFT) all from eBioscience; anti-CD115-PE (clone AFS98), anti-CD62L-PerCP-Cy5.5 (clone MEL-14), anti-CD3-PerCP-Cy5.5 (clone 17A2), anti-major histocompatibility complex II-PerCP-Cy5.5 (clone M5-/114.15.2), anti-CD69-PE-Cy7 (clone H1.2F3), anti-CD25-PE-Cy7 (clone PC61), anti-CD44-APC (clone IM7), anti-Gr-1-APC (clone RB6-8C5), anti-CD11b-BV421 (clone M1/70), anti-CD4-BV421 (clone RM4-5), anti-CD45-BV510 (clone 30-F11), and anti-CD8-BV510 (clone 53-6.7) all from Biolegend (San Diego, CA); anti-Arginase-1-PE from R&D Systems (Minneapolis, MN). Dead cells were excluded with 7AAD (BD Biosciences) or fixable viability dye eFluor 780 (eBioscience) staining. FACS analyses were performed on a FACS Canto II (BD Biosciences). Data analysis was performed using FlowJo software (Tree Star, Ashland, OR).

Pentamer staining of endogeneous CD8^{+} T cells and IFN-γ production

For the detection of endogenous gp100-specific CD8^{+} T cells, we used an H-2K[b]-KVPRNQDWL pentamer (ProImmune, Oxford, UK). Skin and draining LNs were analyzed for the presence of H-2K[b]-KVPRNQDWL pentamer-positive CD8^{+} T cells. The cells were stained according to the manufacturer's protocol, and unspecific pentamer binding was excluded by pregating on viable CD19^{−} (clone 1D3, BD Biosciences) NKp46^{−} (clone 29A1.4, Biolegend) cells. For the detection of IFN-γ, we incubated cell suspensions from draining LNs with 1 μM gp100 peptide (KVPRNQDWL, Pepti-de&Elephants, Potsdam, Germany) for 48 h at 37 °C. IFN-γ release and antibody staining were performed as described above. For the calculation of gp100-responsive IFN-γ^{+} CD8^{+} cells, we used this formula: ((mean of IFN-γ^{+} CD8^{+} cells restimulated with gp100 peptide) − (mean of IFN-γ^{+} CD8^{+} cells cultured without gp100 peptide))/(mean of unstimulated pentamer^{+} CD8^{+} cells).

MDSC suppression assay

For purification of MDSC subsets from tumor tissue, ear and tail skin of 4–5 late-stage tumor mice were digested with 0.15 mg ml^{-1} Liberase (Roche) and 0.12 mg ml^{-1} DNAse (Roche) for 45 min at 37 °C and pressed through 100-μm cell strainers (BD Biosciences). CD45^{+} cells were enriched with a 1.119 g ml^{-1} Histodenz density gradient according to the manufacturer's protocol (Sigma-Aldrich, St. Louis, MO). The grMDSCs and moMDSCs were purified by flow cytometric cell sorting with a FACS Aria as follows: CD45^{+} CD11b^{+} cells were distinguished with Ly-6C and Gr-1 into Gr-1[inter] Ly-6C^{high} moMDSCs and Gr-1^{high} Ly-6C^{low} grMDSCs. CD8^{+} T cells were isolated from LNs and spleen of pmel-1 mice before the onset of spontaneous vitiligo (2–3 months). Purification was performed with anti-mouse-CD8-α (Ly-2) MicroBeads (Miltenyi Biotec, Bergisch Gladbach, Germany). In order to track T-cell proliferation, cells

were stained with 0.4 μM CFSE for 5 min at room temperature. For suppression assays, 1×10^2 BMDCs loaded with 1 μM gp100 peptide (KVPRNQDWL, Peptide&Elephants) for 1 h at 37 °C. These cells were cultured with 2×10^4 CFSE-labeled CD8$^+$ T cells from pmel-1 mice and 2×10^3 or 1×10^4 sorted moMDSCs/grMDSCs for 3 days. T-cell proliferation was measured by analysis of CFSE dilution by flow cytometry.

qPCR analysis of the skin and tumor samples

The total RNA of ear skin, tumor samples, sorted MDSC subsets, CD45$^-$ tumor cells, and CD45$^+$ CD11b$^-$ leukocytes was isolated using TRIzol Reagent (Life Technologies, Carlsbad, CA) according to the manufacturer's instructions and analyzed by electrophoresis on 1.5% agarose gels for RNA integrity (Sigma-Aldrich) after sample preparation in $2 \times$ RNA Loading Dye (Thermo Fischer Scientific, Waltham, MA). Total RNA was reverse transcribed into cDNA with random hexamers and SuperScript II Reverse Transcriptase (Life Technologies). qPCR analysis was performed on a BioRad CFX96 using Brilliant III Ultra-Fast qPCR and qRT-PCR Master Mix (Agilent technologies, Boeblingen, Germany). The following sequences for probes and primers specific for different ligands were purchased from Life Technologies: Mm00475988_m1 (Arginase-1), Mm00440502_m1 (iNOS), and Mm01178820_m1 (TGF-β1). Sequences for probes and primers specific for mouse TATA-binding protein were selected by Primer Express software (Applied Biosystems) and synthesized by Microsynth (Balgach, Switzerland).

Statistical analyses

All experiments involved groups of two to six mice and were performed at least twice with similar results. Statistical analysis was performed using PRISM 5.0 (GraphPad Software, La Jolla, CA). Unpaired Student's *t*-test was used to determine the statistical significance of the mean percentages of cell types between tumor-free and tumor-bearing mice (Figures 2a–c, 3b, 4c, 4d, 5f and h; Supplementary Figure S3, S4 and S6 online). One-way analysis of variance followed by *post hoc* Tukey's test was used to compare means among three or more independent groups (Figures 1a, 1b, 1c, 1e, 4a, 4b and 5a). A *P*-value of <0.05 was considered statistically significant (*), <0.01 very significant (**), and <0.001 highly significant (***). The exact number of mice used per experiment (n = number of mice) is indicated in the corresponding legend of each figure. Error bars represent SEM (bar graph) or range from minimum to maximum values (box and whiskers).

SUPPLEMENTARY MATERIAL
Supplementary material is linked to the online version of the paper at http://www.nature.com/jid

REFERENCES

Ahmadzadeh M, Johnson LA, Heemskerk B *et al.* (2009) Tumor antigen-specific CD8 T cells infiltrating the tumor express high levels of PD-1 and are functionally impaired. *Blood* 114:1537–44

Akbar AN, Henson SM (2011) Are senescence and exhaustion intertwined or unrelated processes that compromise immunity? *Nat Rev Immunol* 11: 289–95

Bakker AB, Schreurs MW, de Boer AJ *et al.* (1994) Melanocyte lineage-specific antigen gp100 is recognized by melanoma-derived tumor-infiltrating lymphocytes. *J Exp Med* 179:1005–9

Becker JC, Houben R, Schrama D *et al.* (2010) Mouse models for melanoma: a personal perspective. *Exp Dermatol* 19:157–64

Boon T, Coulie PG, Van den Eynde BJ *et al.* (2006) Human T cell responses against melanoma. *Annu Rev Immunol* 24:175–208

Burnet M (1957) Cancer; a biological approach. I. The processes of control. *Br Med J* 1:779–86

Chen S, Zhu H, Wetzel WJ *et al.* (1996) Spontaneous melanocytosis in transgenic mice. *J Investig Dermatol Symp Proc* 106:1145–51

Cohen-Solal KA, Reuhl KR, Ryan KB *et al.* (2001) Development of cutaneous amelanotic melanoma in the absence of a functional tyrosinase. *Pigment Cell Res* 14:466–74

Dunn GP, Bruce AT, Ikeda H *et al.* (2002) Cancer immunoediting: from immunosurveillance to tumor escape. *Nature Immunol* 3:991–8

Fourcade J, Sun Z, Benallaoua M *et al.* (2010) Upregulation of Tim-3 and PD-1 expression is associated with tumor antigen-specific CD8+ T cell dysfunction in melanoma patients. *J Exp Med* 207:2175–86

Gabrilovich DI, Nagaraj S (2009) Myeloid-derived suppressor cells as regulators of the immune system. *Nat Rev Immunol* 9:162–74

Gabrilovich DI, Ostrand-Rosenberg S, Bronte V (2012) Coordinated regulation of myeloid cells by tumours. *Nature Rev Immunol* 12:253–68

Gajewski TF, Schreiber H, Fu YX (2013) Innate and adaptive immune cells in the tumor microenvironment. *Nat Immunol* 14:1014–22

Haanen JB, Baars A, Gomez R *et al.* (2006) Melanoma-specific tumor-infiltrating lymphocytes but not circulating melanoma-specific T cells may predict survival in resected advanced-stage melanoma patients. *Cancer Immunol Immunother* 55:451–8

Kawakami Y, Dang N, Wang X *et al.* (2000) Recognition of shared melanoma antigens in association with major HLA-A alleles by tumor infiltrating T lymphocytes from 123 patients with melanoma. *J Immunother* 23:17–27

Kimpfler S, Sevko A, Ring S *et al.* (2009) Skin melanoma development in ret transgenic mice despite the depletion of CD25+Foxp3+ regulatory T cells in lymphoid organs. *J Immunol* 183:6330–7

Klages K, Mayer CT, Lahl K *et al.* (2010) Selective depletion of Foxp3+ regulatory T cells improves effective therapeutic vaccination against established melanoma. *Cancer Res* 70:7788–99

Ladanyi A, Somlai B, Gilde K *et al.* (2004) T-cell activation marker expression on tumor-infiltrating lymphocytes as prognostic factor in cutaneous malignant melanoma. *Clin Cancer Res* 10:521–30

Landsberg J, Gaffal E, Cron M *et al.* (2010) Autochthonous primary and metastatic melanomas in Hgf-Cdk4 R24C mice evade T-cell-mediated immune surveillance. *Pigment Cell Melanoma Res* 23:649–60

Marin YE, Namkoong J, Cohen-Solal K *et al.* (2006) Stimulation of oncogenic metabotropic glutamate receptor 1 in melanoma cells activates ERK1/2 via PKCepsilon. *Cell Signal* 18:1279–86

Motz GT, Coukos G (2013) Deciphering and reversing tumor immune suppression. *Immunity* 39:61–73

Namkoong J, Shin SS, Lee HJ *et al.* (2007) Metabotropic glutamate receptor 1 and glutamate signaling in human melanoma. *Cancer Res* 67:2298–305

Nishikawa H, Sakaguchi S (2010) Regulatory T cells in tumor immunity. *Int J Cancer* 127:759–67

Overwijk WW, Theoret MR, Finkelstein SE *et al.* (2003) Tumor regression and autoimmunity after reversal of a functionally tolerant state of self-reactive CD8+ T cells. *J Exp Med* 198:569–80

Pollock PM, Cohen-Solal K, Sood R *et al.* (2003) Melanoma mouse model implicates metabotropic glutamate signaling in melanocytic neoplasia. *Nat Genet* 34:108–12

Prickett TD, Samuels Y (2012) Molecular pathways: dysregulated glutamatergic signaling pathways in cancer. *Clin Cancer Res* 18:4240–6

Rizzuto GA, Merghoub T, Hirschhorn-Cymerman D *et al.* (2009) Self-antigen-specific CD8+ T cell precursor frequency determines the quality of the antitumor immune response. *J Exp Med* 206:849–66

Rosenberg SA, Yang JC, Restifo NP (2004) Cancer immunotherapy: moving beyond current vaccines. *Nat Med* 10:909–15

Schiffner S, Chen S, Becker JC *et al.* (2012) Highly pigmented Tg(Grm1) mouse melanoma develops non-pigmented melanoma cells in distant metastases. *Exp Dermatol* 21:786–8

Schreiber RD, Old LJ, Smyth MJ (2011) Cancer immunoediting: integrating immunity's roles in cancer suppression and promotion. *Science* 331:1565–70

Senovilla L, Vacchelli E, Galon J *et al.* (2012) Trial watch: prognostic and predictive value of the immune infiltrate in cancer. *Oncoimmunology* 1:1323–43

Umansky V, Abschuetz O, Osen W *et al.* (2008) Melanoma-specific memory T cells are functionally active in Ret transgenic mice without macroscopic tumors. *Cancer Res* 68:9451–8

van Houdt IS, Sluijter BJ, Moesbergen LM *et al.* (2008) Favorable outcome in clinically stage II melanoma patients is associated with the presence of activated tumor infiltrating T-lymphocytes and preserved MHC class I antigen expression. *Int J Cancer* 123:609–15

Vesely MD, Kershaw MH, Schreiber RD *et al.* (2011) Natural innate and adaptive immunity to cancer. *Annu Rev Immunol* 29:235–71

Willimsky G, Blankenstein T (2007) The adaptive immune response to sporadic cancer. *Immunol Rev* 220:102–12

Xiao H, Peng Y, Hong Y *et al.* (2011) Lentivector prime and vaccinia virus vector boost generate high-quality CD8 memory T cells and prevent autochthonous mouse melanoma. *J Immunol* 187:1788–96

Yang L, Pang Y, Moses HL (2010) TGF-beta and immune cells: an important regulatory axis in the tumor microenvironment and progression. *Trends Immunol* 31:220–7

Youn JI, Nagaraj S, Collazo M *et al.* (2008) Subsets of myeloid-derived suppressor cells in tumor-bearing mice. *J Immunol* 181:5791–802

Zea AH, Rodriguez PC, Atkins MB *et al.* (2005) Arginase-producing myeloid suppressor cells in renal cell carcinoma patients: a mechanism of tumor evasion. *Cancer Res* 65:3044–8